



Adaptive fixed-time control with prescribed performance for nonlinear networked control systems under deception attacks*

Linfang Shao¹, Weiwei Sun¹, Lusong Ding¹

Institute of Automation, Qufu Normal University,
Qufu 273165, China
slfslf1116@163.com; wwsun@hotmail.com;
dingls2022@163.com

Received: March 12, 2025 / **Revised:** December 22, 2025 / **Published online:** March 24, 2026

Abstract. This paper presents a novel fixed-time adaptive control scheme with prescribed performance for nonlinear networked control systems (NCSs) under deception attacks. The Nussbaum function is first employed to tackle the challenge of unknown attack weights and their signs. A hybrid approach integrating a fixed-time performance function with a nonlinear shifting function is used to mitigate the influence of initial conditions on tracking errors. Furthermore, a sufficient condition is derived to guarantee the practical fixed-time stability of NCSs, even in the face of deception attacks. Finally, the effectiveness of the proposed methodology is demonstrated through a mass-spring-damper system simulation.

Keywords: deception attacks, fixed-time control, networked control systems, prescribed performance control.

1 Introduction

Networked control systems (NCSs) have become integral to various modern industrial sectors, including smart grids, transportation, and healthcare [13, 23, 26]. These systems rely on digital networks to connect controllers, actuators, and sensors, thereby enabling remote control and resource sharing. However, the open nature of these communication channels makes NCSs highly vulnerable to cyberattacks [1, 6, 10, 28]. Such attacks, including denial-of-service and deception attacks, pose significant risks of performance degradation and potential system instability. Given the increasing prevalence of cyberattacks and the critical role of NCSs in modern infrastructure, addressing these security challenges has become a paramount research area [6, 10, 22]. Ensuring system stability

*This work was supported in part by the Taishan Scholar Project of Shandong Province under grant No. tsqn202211129 and in part by the National Natural Science Foundation of China under grant No. 62073189.

¹Corresponding author.

and reliability under attack conditions is not only a technical necessity but also crucial for safeguarding critical operations in sectors such as smart grids and healthcare. Therefore, developing novel control strategies and security mechanisms to enhance the resilience of NCSs against cyberattacks is both timely and essential.

Deception attacks, characterized by the injection of false information into system signals, pose a significant challenge in NCSs [1, 10, 19, 28]. Deception attacks are notoriously difficult to detect. While adaptive control schemes were proposed to counter deception attacks in NCSs, such as those in [1, 10, 28], they typically ensure only asymptotic stability. In contemporary control theory, there is a need for systems that exhibit convergence to zero within a finite time period, thereby providing a more rapid rate of convergence. However, the calculation of settling time in finite-time control relies on having information about the initial conditions, which obscures the prediction of this duration when initial states remain unspecified. To counter this limitation, fixed-time (FxT) control has gained prominence, providing a consistent settling time irrespective of initial conditions [4, 5, 15]. Building on the work of [16], effective FxT control strategies have been developed across diverse domains, including stochastic nonlinear systems [9], multiagent systems [20], spacecraft systems [3], and NCSs [27], among others. However, a critical gap remains when these strategies are confronted with the pervasive threat of deception attacks. Specifically, most existing results are limited to attacks on a single communication channel (e.g., only sensors or only actuators), which is an oversimplification of real-world threats. The simultaneous occurrence of attacks on both channels introduces coupled uncertainties and, more critically, can lead to an unknown control direction. This phenomenon severely undermines most existing control schemes and makes the design of a controller with a predetermined settling time exceptionally difficult. These intertwined challenges: multichannel attacks, unknown control direction, and the FxT stability requirement have significantly limited the research of FxT secure control results in the literature.

Compounding the stability challenge, the attainment of accurate steady-state tracking and tailored transient responses is imperative for a multitude of practical applications [2, 11, 12, 14, 29]. This requirement for prescribed performance becomes even more stringent under deception attacks, as these attacks can deliberately drive the system states away from desired trajectories, making predefined performance bounds difficult to maintain. To address these tracking performance criteria, the notion of prescribed performance control (PPC) was initially introduced, as detailed in [2]. Building upon the PPC concept, a control strategy was developed using state-observer-based techniques for switched nonlinear systems [12], ensuring that tracking error was confined within a specified region. However, these methods often require the system's initial tracking error to be known within a limited range, which can increase the conservativeness of the control design. This dependency on initial conditions introduces undesirable conservatism into the control design, a limitation that is exacerbated in the hostile and unpredictable environment created by cyberattacks. Fortunately, the limitation of initial condition dependence for tracking error was overcome in [29]. Further advancement in PPC for uncertain nonlinear systems was made in [11], where it was ensured that tracking error was steered to a designated region within a predetermined time frame. Moreover, deception attacks, characterized

by their ability to manipulate data integrity and disrupt system operations, pose significant challenges to NCSs by inducing packet losses and data transmission failures. Consequently, these attacks complicate controller design and highlight the critical need to enhance tracking accuracy and transient performance.

Building on prior discussions, this paper investigates the FxT adaptive PPC problem for nonlinear NCSs under deception attacks. The principal contributions are outlined below:

- (i) In contrast to prior research focusing solely on FxT secure control outcomes limited to deception attacks on a single communication channel, this paper examines a broader scope of deception attacks occurring on two communication channels for nonlinear NCSs.
- (ii) This paper is the inaugural investigation into the PPC issue for nonlinear NCSs subjected to two communication channels deception attacks in a FxT frame. The suggested fixed-time performance function (FxTPF) enhances dynamic response, constrains peak overshoot, and consistently maintains tracking errors within pre-defined limits.
- (iii) In contrast to the conventional approach for addressing PPC issues, we construct a novel method involving a nonlinear shifting function (NSF) and a FxTPF, removing the constraint associated with the tracking error being influenced by the initial conditions. Consequently, the level of conservatism in the design approach we have formulated is minimized.

2 Problem formulation and preliminaries

2.1 System description

Consider the following uncertain nonlinear NCSs:

$$\begin{aligned}\dot{x}_i &= x_{i+1} + h_i(t)\phi_i(\bar{x}_i), \quad i = 1, 2, \dots, n-1, \\ \dot{x}_n &= \tilde{u} + h_n(t)\phi_n(\bar{x}_n), \\ y &= x_1,\end{aligned}\tag{1}$$

where $\bar{x}_i = [x_1, x_2, \dots, x_i]^T \in \mathbb{R}^i$, x_i represents the system state, which is unavailable. $\tilde{u} \in \mathbb{R}$ is the attacked system input. The system output y and the unknown parameter $h_i(t)$ are both elements of \mathbb{R} . Additionally, $\phi_i : \mathbb{R} \rightarrow \mathbb{R}$, $i = 1, 2, \dots, n$, represents a set of known smooth nonlinear functions.

Deception attacks are typically understood as assaults targeting sensor and actuator, with the attack being conceptualized as follows:

$$\begin{aligned}\tilde{x}_i(t) &= x_i(t) + \delta_s(t, x_i(t)), \quad i = 1, 2, \dots, n, \\ \tilde{u}(t) &= a(t)u(t) + \delta_a(t, \bar{x}_n(t)),\end{aligned}\tag{2}$$

where the compromised system state after a sensor attack is denoted as $\tilde{x}_i(t)$, $u(t)$ represents the designed control signal. The sensor data is subject to an attack signal denoted

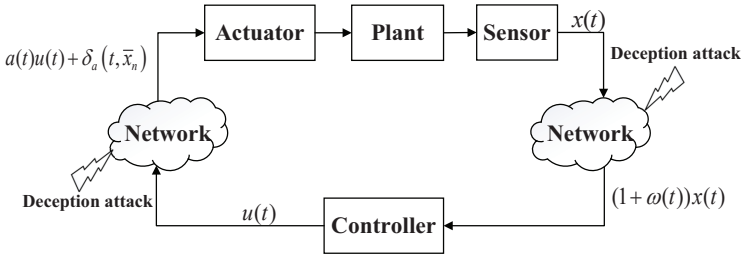


Figure 1. Schematic representation of deception attacks.

by $\delta_s(t, x_i(t))$, where $\delta_s(t, x_i(t)) = \omega_i(t)x_i(t)$, here $\omega_i(t)$ represents an unknown coefficient [1]. An unknown sign multiplicative actuator attack gain is denoted by $a(t)$, the term $\delta_a(t, \bar{x}_n(t))$ signifies the erroneous data superimposed onto the actuator’s control input [10]. The constant threat of malicious deception attacks on the considered NCSs is illustrated in Fig. 1.

Assumption 1. (See [1].) The coefficient $\omega_i(t)$ adheres to the specified conditions

$$\omega_i(t) \neq -1.$$

Assumption 2. The time-varying gains represented by $a(t)W_n$ and $W_i\lambda_{i+1}^{-1}$ are bounded.

Remark 1. Equation (2) facilitates expression $\tilde{x}_i(t)$ in terms of $\tilde{x}_i(t) = (1 + \omega_i(t))x_i(t)$. When $\omega_i(t) = -1$, the attack nullifies the system state, leading to $\tilde{x}_i(t) = 0$. In such cases, the restoration of desired system performance and stability through the construction of $u(t)$ becomes unattainable. Therefore, it is imperative that $1 + \omega_i(t) \neq 0$. To simplify the notation, let $\mu_i = W_iW_{i+1}^{-1}$, $W_i(t) = 1 + \omega_i(t)$, then $\tilde{x}_i(t) = W_i(t)x_i(t) \triangleq W_i x_i(t)$.

Remark 2. The potential for loss of control direction as a result of deception attacks is a significant concern. This paper explores the application of the Nussbaum function scheme as a strategy to address the control design challenges posed by such attacks. Therefore, it is imperative to proactively address this issue. The Nussbaum function $N_k(\chi_k)$ proposed in this paper is $N_k(\chi_k) = e^{\chi_k^2} \cos(\chi_k\pi)$, $k = 1, \dots, n$.

Lemma 1. (See [17].) For system

$$\dot{s} = \gamma(t, s), \quad s(0) = s_0, \tag{3}$$

where $\gamma : \mathbb{R}^+ \times \mathbb{R}^n \rightarrow \mathbb{R}^n$ represents a continuously differentiable function with the requisite properties $\gamma(0, 0) = 0$, $s \in \mathbb{R}^n$ denotes the state of (3). If a continuously differentiable function $V(s)$ exists, it is radially unbounded and exhibits positive definiteness such that

$$\begin{aligned} r_1(\|s(t)\|) &\leq V(s(t)) \leq r_2(\|s(t)\|), \\ \dot{V}(s) &\leq -aV^\tau(s) - bV^\beta(s) - cV(s) + k, \end{aligned}$$

where r_1 and r_2 are class \mathcal{K}_∞ functions, $0 < \beta < 1$, $a, b, c, k > 0$, $\tau > 1$, then system (3) exhibits practical fixed-time stable (PFxTS).

Lemma 2. (See [8].) Let $\xi(\cdot)$ and $V(\cdot)$ be differentiable functions defined on $[0, t_m)$, and let $V(t) \geq 0$. Suppose that $N(\chi)$ is a smooth Nussbaum function satisfying the inequality

$$V(t) \leq v_0 + e^{-v_1 t} \int_0^t (f(\tau)N(\chi(\tau)) + 1) \dot{\chi}(\tau) e^{v_1 \tau} d\tau$$

for all $t \in [0, t_m)$, where v_0 denotes a constant of relevance, v_1 is a positive constant, $f(t)$ is a variable that falls within the range of $[h_1, h_2]$, where h_1 and h_2 are constants satisfying either $0 < h_1 < h_2$ or $0 > h_2 > h_1$. Then $V(t)$, $\int_0^t g(\tau)N(\chi(\tau))\dot{\chi}(\tau) d\tau$, and $\chi(t)$ are bounded over $[0, t_m)$.

Lemma 3. (See [24].) The unknown nonlinear function $F_i(\Lambda_i)$ is estimated using neural networks (NNs)

$$F_i(\Lambda_i) = P_i^* \Gamma H_i(\Lambda_i) + \varepsilon_i, \quad |\varepsilon_i| \leq \bar{\varepsilon}_i,$$

where $H_i(\Lambda_i)$ indicates the basis function vector, P_i^* is the ideal weight vector, ε_i is the approximation error, $|\varepsilon_i| \leq \bar{\varepsilon}_i$, with $\bar{\varepsilon}_i$ being a positive constant, $P_i = \|P_i^*\|^2$, \hat{P}_i represents the estimation of P_i , and $\tilde{P}_i = P_i - \hat{P}_i$.

2.2 Fixed-time performance function

We construct a FxTPF as follows:

$$\Phi(t) = \begin{cases} (1-r)\left(\frac{1}{2\pi} \sin \frac{2\pi t}{T_c} + \frac{T_c-t}{T_c}\right) + r, & 0 \leq t < T_c, \\ r, & t \geq T_c, \end{cases} \quad (4)$$

where $0 < r \leq 1$ is a parameter that needs to be designed, T_c is the setting time.

Remark 3. According to (4), the function $\Phi(t)$ possesses the following properties:

- (i) $\Phi(t) > 0$ and $\dot{\Phi}(t) \leq 0$;
- (ii) $\lim_{t \rightarrow T_c} \Phi(t) = r$;
- (iii) $\Phi(t) = r$ for all $t \geq T_c$.

These properties imply that $\Phi(t)$ is continuous for $t \geq 0$, as the limit exists at $t = T_c$ and the function remains constant thereafter.

2.3 Control objective

The objective of this paper is to design a controller that is both adaptable and robust, ensuring that the nonlinear NCSs (1) exhibit PFxTS and that all signals within the closed-loop system remain bounded even in the presence of malicious attacks as described in (2). Meanwhile, the designed controller should guarantee that the system's tracking error converges to a predefined constraint region within a specified time frame, regardless of the initial conditions.

3 Main result

This section outlines the formulation of an adaptive FxT secure control strategy designed to achieve control objectives, while ensuring the stability of the system.

3.1 Controller design

The coordinate transformation and NSF are defined as:

$$z_1 = \frac{\zeta(t)}{(p_1 + \zeta(t))(p_2 - \zeta(t))}, \tag{5}$$

$$z_i = \tilde{x}_i - \alpha_{if}, \quad i = 2, \dots, n, \tag{6}$$

and

$$s(z) = \frac{p_1 p_2 (e^z - 1)}{p_2 + p_1 e^z},$$

where $\zeta(t) = s(z(t))/\Phi(t)$, and $p_1, p_2 > 0$ are constants. Clearly, the function $s(z)$ is strictly monotonically increasing over its domain $(-\infty, \infty)$ and maps to the interval $(-p_1, p_2)$, and $z(0) \in \mathbb{R}$. α_{if} can be derived by the filter

$$T_i \dot{\alpha}_{if} + (\alpha_{if} - \alpha_{i-1})^{2\tau-1} + \alpha_{if} = \alpha_{i-1}, \quad i = 2, \dots, n, \tag{7}$$

where $\tau > 1$, $\alpha_{i-1}, \alpha_{if}$ denote the input and output of the filter, the parameter $T_i > 0$ is a design parameter. The filter error is $e_i = \alpha_{if} - \alpha_{i-1}, i = 2, \dots, n$. Based on (7), one has

$$\dot{e}_i = -\frac{e_i}{T_i} - \frac{e_i^{2\tau-1}}{T_i} + \mathfrak{S}_{i-1}, \quad i = 2, \dots, n,$$

where

$$\mathfrak{S}_1 = -\frac{\partial \tau_1}{\partial z_1} \dot{z}_1 - \frac{\partial \tau_1}{\partial \hat{P}_1} \dot{P}_1 - \frac{\partial \tau_1}{\partial v_1} \dot{v}_1 - \frac{\partial \tau_1}{\partial \chi_1} \dot{\chi}_1,$$

and for $i = 2, \dots, n - 1$,

$$\mathfrak{S}_i = -\frac{\partial \tau_i}{\partial z_i} \dot{z}_i - \frac{\partial \tau_i}{\partial \hat{P}_i} \dot{P}_i - \frac{\partial \tau_i}{\partial \chi_i} \dot{\chi}_i.$$

For $A, B, C > 0$, define compact sets Ω_d, Ω_Φ , and Ω_V as follows:

$$\Omega_d := \{[y_d, \dot{y}_d, \ddot{y}_d]^T: y_d^2 + \dot{y}_d^2 + \ddot{y}_d^2 \leq A\} \subset \mathbb{R}^3,$$

$$\Omega_\Phi := \{[\Phi, \dot{\Phi}]^T: \Phi^2 + \dot{\Phi}^2 \leq B\} \subset \mathbb{R}^2,$$

and

$$\Omega_V := \left\{ \sum_{i=1}^n z_i^2 + \sum_{i=1}^n \frac{1}{l_i} \tilde{P}_i^2 + \sum_{i=2}^n e_i^2 \leq 2C \right\} \subset \mathbb{R}^{3n-1}.$$

Then there is a positive constant \mathcal{K}_i such that $|\mathfrak{S}_i| \leq \mathcal{K}_i$ on $\Omega_d \times \Omega_\Phi \times \Omega_V$.

Using the previously established coordinate transformation and the first-order filter, the FxT controller is formulated as follows.

Step 1. By employing (5), we can determine \dot{z}_1 as

$$\dot{z}_1 = v_1(\dot{\tilde{x}}_1 - \dot{y}_d) + v_2 = v_1(\mu_1(z_2 + e_2 + \alpha_1) + f_1 - \dot{y}_d) + v_2,$$

where y_d is the desired signal, and

$$v_1 = \frac{\lambda\rho}{\Phi(t)}, \quad v_2 = -\frac{\lambda s(z)\dot{\Phi}(t)}{\Phi^2(t)}, \quad \lambda = \frac{p_1 p_2 + \zeta^2(t)}{(p_1 + \zeta(t))^2(p_2 - \zeta(t))^2},$$

$$f_1 = h_1(t)W_1\phi_1(\tilde{x}_1) + \dot{W}_1W_1^{-1}\tilde{x}_1, \quad \rho = \frac{(p_1 + p_2)p_1 p_2 e^z}{(p_2 + p_1 e^z)^2}.$$

Take the Lyapunov function as

$$V_1 = \frac{1}{2}z_1^2 + \frac{1}{2l_1}\tilde{P}_1^2 + \frac{1}{2}e_2^2. \tag{8}$$

Then

$$\dot{V}_1 = z_1(v_1(\mu_1(z_2 + e_2 + \alpha_1) + f_1 - \dot{y}_d) + v_2) - \frac{1}{l_1}\tilde{P}_1\dot{\tilde{P}}_1 + e_2\dot{e}_2.$$

By employing Young’s inequality in conjunction with (8), it can be deduced that

$$\dot{V}_1 \leq z_1\left(v_1(\mu_1 z_2 + f_1 \dot{y}_d) + v_2 + v_1 \mu_1 \alpha_1 + \frac{1}{2}z_1 v_1^2 \mu_1^2\right) + \frac{1}{2}e_2^2 - \frac{1}{l_1}\tilde{P}_1\dot{\tilde{P}}_1 + e_2\dot{e}_2. \tag{9}$$

Let $F_1 = v_1(\mu_1 z_2 + f_1 - \dot{y}_d) + z_1 v_1^2 \mu_1^2 / 2 + v_2$, F_1 is approximated using NNs.

Design α_1 , parameter update law of \tilde{P}_1 , and χ_1 as follows:

$$\alpha_1 = N(\chi_1)\frac{z_1\zeta_1^2}{v_1\sqrt{z_1^2\zeta_1^2 + \epsilon_1^2}}, \tag{10}$$

$$\dot{\tilde{P}}_1 = \frac{l_1}{2J_1^2}z_1^2 H_1^T H_1 - \sigma_{11}\tilde{P}_1 - \sigma_{12}\hat{P}_1^{2\tau-1}, \tag{11}$$

$$\dot{\chi}_1 = \frac{z_1^2\zeta_1^2}{\sqrt{z_1^2\zeta_1^2 + \epsilon_1^2}},$$

where

$$\zeta_1 = c_1 z_1 + d_1 z_1^{2\tau-1} + q_1 z_1^{2\beta-1} + \frac{z_1}{2} + \frac{1}{2J_1^2}z_1 H_1^T H_1 \hat{P}_1$$

in which $c_1, d_1, J_1, \epsilon_1, l_1, \sigma_{11}, \sigma_{12} > 0$ and $\tau > 1$ are parameters that need to be designed.

Upon substituting (10)–(11) into (9) and leveraging Young’s inequality, it becomes evident that

$$\dot{V}_1 \leq -c_1 z_1^2 - d_1 z_1^{2\tau} - q_1 z_1^{2\beta} + (\mu_1 N(\chi_1) + 1)\dot{\chi}_1 + \frac{\sigma_{11}}{l_1}\tilde{P}_1\hat{P}_1 + \frac{\sigma_{12}}{l_1}\tilde{P}_1\hat{P}_1^{2\tau-1} + \frac{J_1^2 + \bar{\epsilon}_1^2}{2} + \epsilon_1 - \left(\frac{1}{T_2} - 1\right)e_2^2 - \frac{1}{T_2}e_2^{2\tau} + \frac{1}{2}\mathfrak{S}_1.$$

Step k : $2 \leq k \leq n - 1$. Based on (6),

$$\dot{z}_k = \mu_k(z_{k+1} + e_{k+1} + \alpha_k) + f_k - \dot{\alpha}_{kf},$$

where $f_k = h_k(t)W_k\phi_k(\bar{x}_k) + \dot{W}_k W_k^{-1}\tilde{x}_k$.

Construct the Lyapunov function as

$$V_k = \frac{1}{2}z_k^2 + \frac{1}{2l_k}\tilde{P}_k^2 + \frac{1}{2}e_{k+1}^2.$$

Differentiating V_k will give

$$\dot{V}_k \leq z_k(\mu_k(z_{k+1} + e_{k+1} + \alpha_k) + f_k - \dot{\alpha}_{kf}) - \frac{1}{l_k}\tilde{P}_k\dot{\tilde{P}}_k + e_{k+1}\dot{e}_{k+1}. \tag{12}$$

By employing Young’s inequality in conjunction with (12), we obtain

$$\begin{aligned} \dot{V}_k &\leq z_k\left(\mu_k(z_{k+1} + \alpha_k) + f_k + \frac{1}{2}z_k\mu_k^2\dot{\alpha}_{kf}\right) - \frac{1}{l_k}P_k\dot{\tilde{P}}_k + \frac{1}{2}e_{k+1}^2 \\ &\quad + e_{k+1}\dot{e}_{k+1}. \end{aligned} \tag{13}$$

Let $F_k = \mu_k z_{k+1} + f_k - \dot{\alpha}_{kf} + z_k \mu_k^2 / 2$, and F_k is approximated using NNs.

Design α_k , parameter update law of \hat{P}_k , and χ_k as follows:

$$\alpha_k = N(\chi_k) \frac{z_k \zeta_k^2}{v_k \sqrt{z_k^2 \zeta_k^2 + \epsilon_k^2}}, \tag{14}$$

$$\dot{\tilde{P}}_k = \frac{l_k}{2J_k^2} z_k^2 H_k^T H_k - \sigma_{k1} \tilde{P}_k - \sigma_{k2} \tilde{P}_k^{2\tau-1}, \tag{15}$$

$$\dot{\chi}_k = \frac{z_k^2 \zeta_k^2}{\sqrt{z_k^2 \zeta_k^2 + \epsilon_k^2}},$$

where

$$\zeta_k = c_k z_k + d_k z_k^{2\tau-1} + q_k z_k^{2\beta-1} + \frac{z_k}{2} + \frac{1}{2J_k^2} z_k H_k^T H_k \tilde{P}_k$$

in which $c_k, d_k, J_k, \epsilon_k, l_k, \sigma_{k1}, \sigma_{k2} > 0$ and $\tau > 1$ are parameters that need to be designed.

Upon substituting (14)–(15) into (13) and leveraging Young’s inequality, it becomes evident that

$$\begin{aligned} \dot{V}_k &\leq -c_k z_k^2 - d_k z_k^{2\tau} - q_k z_k^{2\beta} + (\mu_k N(\chi_k) + 1)\dot{\chi}_k + \frac{\sigma_{k1}}{l_k}\tilde{P}_k\dot{\tilde{P}}_k + \frac{\sigma_{k2}}{l_k}\tilde{P}_k\dot{\tilde{P}}_k^{2\tau-1} \\ &\quad + \frac{J_k^2 + \bar{\epsilon}_k^2}{2} + \epsilon_k - \left(\frac{1}{T_{k+1}} - 1\right)e_{k+1}^2 - \frac{1}{T_{k+1}}e_{k+1}^{2\tau} + \frac{1}{2}\mathfrak{S}_k^2. \end{aligned}$$

Step n . In the event of deception attacks compromising the communication channel connecting the controller and actuator, a secure control scheme is devised as detailed in the following.

The Lyapunov function is constructed by

$$V_n = \frac{1}{2}z_n^2 + \frac{1}{2l_n}\tilde{P}_n^2.$$

Differentiating V_n and proceeding as in $(n - 1)$ th step, we obtain

$$\dot{V}_n \leq z_n(a(t)W_n u(t) + F_n) - \frac{1}{l_n}\tilde{P}_n^2, \tag{16}$$

where

$$F_n = W_n\delta_a(t, \bar{x}_n) + h_n(t)W_n\phi_n(\bar{x}_n) + \dot{W}_nW_n^{-1}\tilde{x}_n - \dot{\alpha}_{nf},$$

F_n is approximated using NNs.

Design the FxT controller $u(t)$, the parameter update law of \hat{P}_n , and χ_n as follows:

$$u = N(\chi_n)\frac{z_n\zeta_n^2}{v_n\sqrt{z_n^2\zeta_n^2 + \epsilon_n^2}}, \tag{17}$$

$$\dot{\hat{P}}_n = \frac{l_n}{2J_n^2}z_n^2H_n^T H_n - \sigma_{n1}\hat{P}_n - \sigma_{n2}\hat{P}_n^{2\tau-1}, \tag{18}$$

$$\dot{\chi}_n = \frac{z_n^2\zeta_n^2}{\sqrt{z_n^2\zeta_n^2 + \epsilon_n^2}},$$

where

$$\zeta_n = c_n z_n + z_n^{2\tau-1} + q_n z_n^{2\beta-1} + \frac{z_n}{2} + \frac{1}{2J_n}z_n H_n^T H_n \hat{P}_n$$

in which $c_n, b_n, J_n, \epsilon_n, \tau > 1, l_n, \sigma_{n1}$, and σ_{n2} are positive design parameters.

Substituting (17)–(18) into (16) and leveraging Young’s inequality, we obtain

$$\begin{aligned} \dot{V}_n \leq & -c_n z_n^2 - d_n z_n^{2\tau} - q_n z_n^{2\beta} + (a(t)W_n N(\chi_n) + 1)\dot{\chi}_n + \epsilon_n \\ & + \frac{\sigma_{n1}}{l_n}\tilde{P}_n\hat{P}_n + \frac{\sigma_{n2}}{l_n}\tilde{P}_n\hat{P}_n^{2\tau-1} + \frac{J_n^2 + \epsilon_n^2}{2}. \end{aligned}$$

3.2 Stability analysis

Theorem 1. *In the context of nonlinear NCSs (1) subject to deception attacks (2), filter (7), FxT controller (17), and adaptive laws (11), (15), along with (18), collectively ensure the PFxTS of the closed-loop system. This design ensures that the tracking error converges to a constrained region within a specified time frame for any initial condition $z(0) \in \mathbb{R}$.*

Proof. To assess the stability of the entire system, the subsequent Lyapunov function is chosen for analysis:

$$V = \sum_{j=1}^n V_j.$$

Using [18, Lemma A.2] and [25, Lemmas 3 and 4], we obtain

$$\begin{aligned} \dot{V} &\leq \sum_{j=1}^n \left(-c_j z_j^2 - d_j z_j^{2\tau} - q_j z_j^{2\beta} + \frac{\sigma_{j1}}{l_j} \tilde{P}_j \hat{P}_j + \frac{\sigma_{j2}}{l_j} \tilde{P}_j \hat{P}_j^{2\tau-1} + \frac{J_j^2 + \bar{\epsilon}_j^2}{2} + \epsilon_j \right) \\ &\quad + (a(t)W_n N(\chi_n) + 1) \dot{\chi}_n \\ &\quad + \sum_{j=1}^{n-1} \left((\mu_j N(\chi_j) + 1) \dot{\chi}_j - \left(\frac{1}{T_{j+1}} - 1 \right) e_{j+1}^2 - \frac{1}{T_{j+1}} e_{j+1}^{2\tau} + \frac{1}{2} \mathfrak{S}_j^2 \right) \\ &\leq \sum_{j=1}^n (-c_j^* V_j - d_j^* V_j^\tau - q_j^* V_j^\beta) + \sum_{j=1}^{n-1} ((\mu_j N(\chi_j) + 1) \chi_j + L_j) \\ &\quad + (a(t)W_n N(\chi_n) + 1) \dot{\chi}_n, \end{aligned}$$

where

$$\begin{aligned} c_j^* &= \min \left\{ 2c_j, \frac{\sigma_{j1}}{2}, \frac{1}{T_{j+1}} - 1 \right\}, & d_j^* &= 3^{1-\tau} \min \left\{ 2^\tau d_j, \frac{(2\tau - 1)\sigma_{j2}}{\tau}, \frac{2^\tau}{T_{j+1}} \right\}, \\ q_j^* &= \min \left\{ 2^\beta q_j, \frac{\sigma_{j1}}{2}, \frac{1}{T_{j+1}} - 1 \right\}, \\ L_j &= \frac{\sigma_{j1}}{2l_j} P_j^2 + \frac{(2\tau - 1)\sigma_{j2}}{2\tau l_j} P_j^{2\tau} + \left(\frac{\sigma_{j1}}{2} + \frac{1}{T_{j+1}} - 1 \right) (1 - \beta) \beta^{\beta/(1-\beta)} \\ &\quad + \epsilon_j + \frac{J_j^2 + \bar{\epsilon}_j^2}{2} + \frac{1}{2} \mathcal{K}_j^2 \end{aligned}$$

for $j = 1, 2, \dots, n - 1$, and

$$\begin{aligned} c_n^* &= \min \left\{ 2c_n, \frac{\sigma_{n1}}{2} \right\}, & d_n^* &= 3^{1-\tau} \min \left\{ 2^\tau d_n, \frac{(2\tau - 1)\sigma_{n2}}{\tau} \right\}, \\ q_n^* &= \min \left\{ 2^\beta q_n, \frac{\sigma_{n1}}{2} \right\}, \\ L_n &= \frac{\sigma_{n1}}{2l_n} P_n^2 + \frac{(2\tau - 1)\sigma_{n2}}{2\tau l_n} P_n^{2\tau} + \frac{\sigma_{n1}}{2} + \epsilon_n + \frac{J_n^2 + \bar{\epsilon}_n^2}{2}. \end{aligned}$$

By invoking Assumption 2, we can establish the boundedness of V_j, χ_j . Combining this with the definition of $\dot{\chi}_j$ indicates that $(\mu_j N(\chi_j) + 1) \chi_j$ and $(a(t)W_n N(\chi_n) + 1) \dot{\chi}_n$ is bounded.

Thus, one has $|(\mu_j N(\chi_j) + 1) \chi_j| \leq \bar{\chi}_j$ and $|(a(t)W_n N(\chi_n) + 1) \dot{\chi}_n| \leq \bar{\chi}_n$ in which $\bar{\chi}_j > 0, j = 1, 2, \dots, n$, is a scalar. Consequently, we derive

$$\dot{V} \leq -cV - dV^\tau - qV^\beta + L, \tag{19}$$

where $c = \min\{c_j^*\}, d = \min\{d_j^*\}, q = \min\{q_j^*\}$, and $L = \sum_{j=1}^n L_j^*, L_j^* = L_j + \bar{\chi}_j, j = 1, 2, \dots, n$.

Accordingly, by applying Lemma 1, we deduce that system (1) exhibits PFxTS, with all system signals remaining bounded. Furthermore, the signal z_1 is proven to be bounded, and it is demonstrated that regardless of the initial value $z(0) \in \mathbb{R}$, the tracking error will eventually approach a predetermined range within a specified time period T_c . \square

Remark 4. Drawing on (19) and Lemma 1, the convergence rate and tracking accuracy are governed primarily by the parameters $c_j, d_j, q_j, l_j, \epsilon_j,$ and T_j . Increasing c_j, d_j, q_j while reducing l_j, ϵ_j, T_j accelerates convergence and improves tracking; the opposite adjustment degrades performance. However, excessive enlargement of c_j, d_j, q_j induces unnecessarily large control inputs, impeding practical implementation. Therefore, these parameters should be chosen judiciously to balance rapidity and feasibility.

4 Simulation

This section introduces a mass-spring-damper system as a case study to demonstrate the efficacy of the proposed control strategy. The system under consideration is modeled as [14]

$$\begin{aligned} \dot{x}_1 &= f_1(x_1)x_2, \\ \dot{x}_2 &= f_2(x_1, x_2)u - \frac{1}{h}g(x_1, x_2), \\ y &= x_1 \end{aligned}$$

in which

$$\begin{aligned} f_1(x_1) &= 6 + 2 \cos x_1, & f_2(x_1, x_2) &= 2 + \sin(x_1x_2^2), \\ g(x_1, x_2) &= 2x_1^2 + x_1^3 \sin(x_1x_2) + 0.2x_2^2 \cos x_2^2, & \text{and } h &= \frac{1}{3}. \end{aligned}$$

The reference signal $y_d = \sin(0.05t)$. The FxTPF $\Phi(t)$ within a FxT $T_c = 3$ s is chosen as follows:

$$\Phi(t) = \begin{cases} 0.9\left(\frac{1}{2\pi} \sin \frac{2\pi t}{3} + \frac{3-t}{T_c}\right) + 0.1, & 0 \leq t < 3, \\ 0.1, & t \geq 3. \end{cases}$$

The design parameters and initial values are selected by $c_1 = c_2 = 8, d_1 = d_2 = 6, q_1 = q_2 = 10, J_1 = J_2 = 0.5, l_1 = l_2 = 0.01, \epsilon_1 = \epsilon_2 = 2, \sigma_{11} = \sigma_{12} = \sigma_{21} = \sigma_{22} = 0.6, T_2 = 0.001, \tau = 5/3,$ and $\beta = 9/11, \hat{P}_1(0) = \hat{P}_2(0) = 0, x_1(0) = 0.1, x_2(0) = 0.1, \chi_1(0) = \chi_2(0) = 0.$

In mass-spring-damper systems, control signals and sensor data are typically transmitted over a network. If an attacker is able to tamper with this data, it could result in degraded or unstable system performance. Specifically, an attacker can falsify sensor data so that the controller receives incorrect displacement or speed information, resulting in a miscalculation of the control signal. In addition, an attacker can tamper with the signal sent from the controller to the actuator, causing the actuator to output the wrong force, which in turn affects the dynamic behavior of the system. Here the signal representing sensor attack is selected as

$$\delta_s(t, x_1(t)) = (-0.2 - 0.15 \cos t)x_1, \quad \delta_s(t, x_2(t)) = (-0.1 - 0.05 \cos t)x_2.$$

The signal representing actuator attack is selected as

$$a(t) = -2 \sin(5t), \quad \delta_a(t, \bar{x}_2(t)) = 2x_1x_2.$$

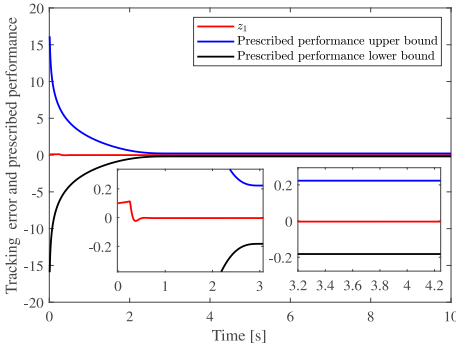


Figure 2. The curves of z_1 and prescribed performance.

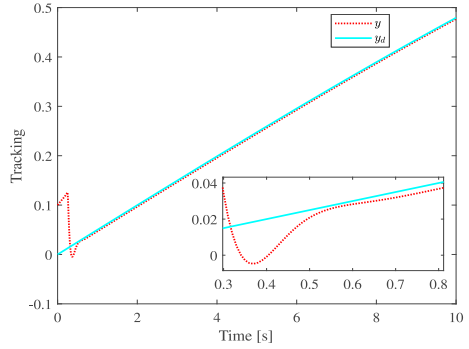


Figure 3. The curves of tracking performance.

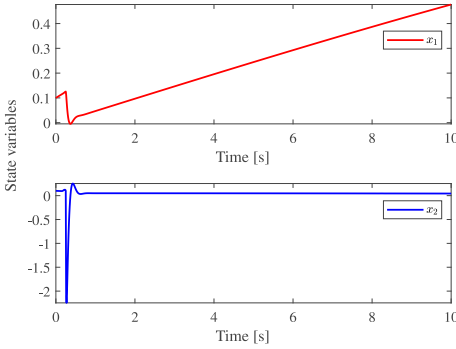


Figure 4. The curves of states.

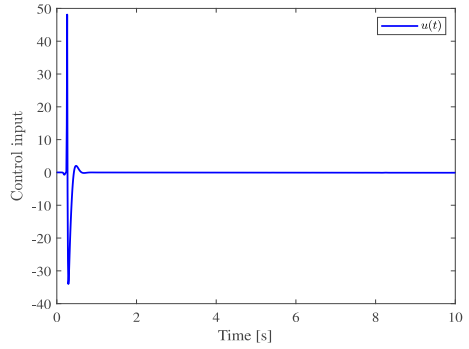


Figure 5. The curve of control input.

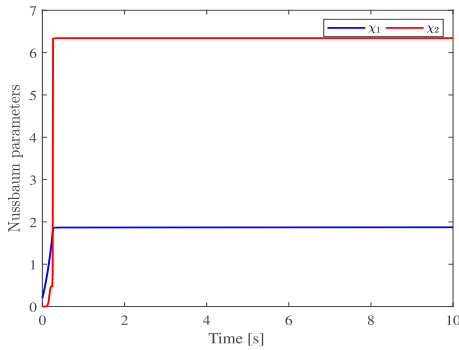


Figure 6. The curves of Nussbaum parameters.

The simulation outcomes are depicted in Figs. 2–6. Figure 2 displays the tracking error of the system under the designed control scheme and the achieved performance constraint bounds following deception attacks. The behaviors of the variable y and its reference signal y_d are depicted in Fig. 3. The dynamics of the state variables x_1, x_2 and

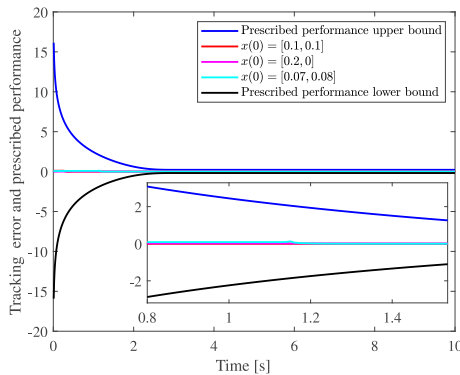


Figure 7. The curves of tracking error and prescribed performance bounds under different initial conditions.

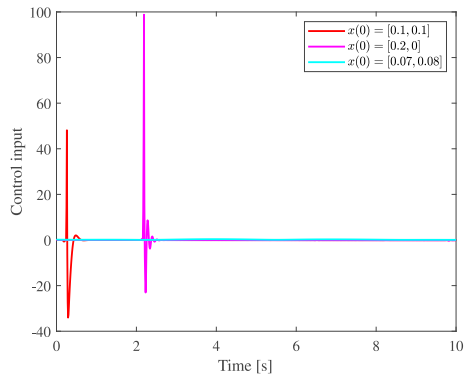


Figure 8. The curves of control input under different initial conditions.

the control input $u(t)$ are illustrated in Figs. 4 and 5, respectively. Figure 6 shows the progression of the Nussbaum function parameters.

To verify the effectiveness of the FxT control, the simulation is conducted under different initial conditions $x(0) = [x_1(0), x_2(0)] = [0.1, 0.1]$, $x(0) = [x_1(0), x_2(0)] = [0.2, 0]$ and $x(0) = [x_1(0), x_2(0)] = [0.07, 0.08]$. Then, under the same controller parameters, the simulation results are shown in Figs. 7 and 8, which indicate effective tracking, highlighting that the system’s tracking error z_1 converges to a prescribed performance constrained bounds within $T_c = 3$ s, irrespective of the initial conditions. This confirms the efficacy of the proposed FxT resilient control strategy.

To further demonstrate the superiority of the designed control strategy in this paper, we employ the following two control design schemes. Scheme I is the FxT adaptive PPC algorithm based on a switched virtual controller proposed in this paper. Scheme II is the FxT control algorithm developed in [7] without considering the system is subject to deception attacks. Scheme III is the tracking control algorithm developed in [21] without considering the system is subject to deception attacks within FxT frame.

The comparative simulation results are displayed in Figs. 9 and 10. Specifically, Fig. 9 shows the tracking error and performance constraint effect under different schemes. The tracking error of Scheme II exceeds the prescribed performance bounds of this paper at 5.1 s, compared with Schemes II and III, the method used in this paper converges faster and the tracking error is smaller. Figure 10 depicts the control input under different schemes. It is clear that a singularity occurs when using the Scheme II, while this problem does not arise with the help of Scheme I. Compared with Scheme III, the method used in this paper has smaller control input, which can improve the stability of the system. In conclusion, the FxT control algorithm proposed in this paper not only avoids the singularity problem found in [7], but also ensures that the tracking error is constrained in a prescribed region. This shows the superiority of the control algorithm proposed in this paper. Thus, the availability and superiority of the constructed adaptive FxT PPC approach in this paper are illustrated by analyzing the simulation results.

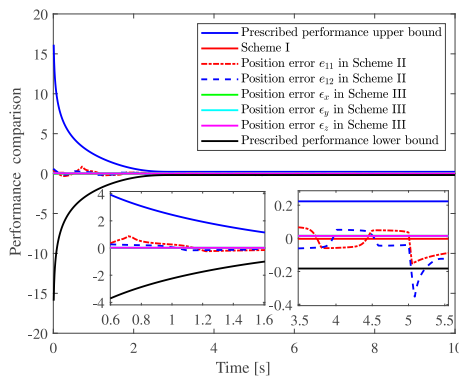


Figure 9. The curves of prescribed performance comparison.

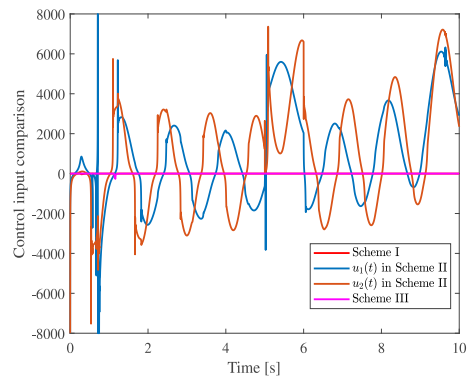


Figure 10. The curves of control input comparison.

5 Conclusion

The development of an adaptive FxT PPC controller that incorporates the dynamic surface control technique and the Nussbaum function for nonlinear NCSs vulnerable to deception attacks has been presented in this paper. The uncertain nonlinear functions have been addressed through NNs. Additionally, NSF and FxTPF have been introduced to mitigate the tracking error limitation on the initial condition. The designed controller effectively compensated for unknown deception attacks, resulting in the compromised nonlinear NCSs being PFxTS. Future research will investigate the implementation of an adaptive prescribed-time control strategy for NCSs in the presence of deception attacks.

Author contributions. All authors (L.S., W.S., and L.D.) have contributed as follows: conceptualization, L.S., W.S., and L.D.; formal analysis, L.D.; investigation, L.S. and W.S.; methodology, W.S.; resources, W.S.; software, W.S. and L.D.; validation, L.S. and L.D.; writing – original draft preparation, L.S.; writing – review & editing, L.S., W.S., and L.D. All authors have read and approved the published version of the manuscript.

Conflicts of interest. The authors declare no conflicts of interest.

References

1. L. An, G.-H. Yang, Improved adaptive resilient control against sensor and actuator attacks, *Inf. Sci.*, **423**:145–156, 2018, <https://doi.org/10.1016/j.ins.2017.09.042>.
2. C. P. Bechlioulis, G. A. Rovithakis, Robust adaptive control of feedback linearizable MIMO nonlinear systems with prescribed performance, *IEEE Trans. Autom. Control*, **53**(9):2090–2099, 2008, <https://doi.org/10.1109/TAC.2008.929402>.
3. Q. Chen, S. Xie, X. He, Neural-network-based adaptive singularity-free fixed-time attitude tracking control for spacecrafts, *IEEE Trans. Cybern.*, **51**(10):5032–5045, 2021, <https://doi.org/10.1109/TCYB.2020.3024672>.

4. X. Chen, W. Sun, X. Gao, D. Yu, Practical fixed-time stabilization for discrete-time impulsive switched port-controlled Hamiltonian systems, *Nonlinear Anal. Model. Control*, **29**(2):349–364, 2024, <https://doi.org/10.15388/namc.2024.29.34648>.
5. G. Cui, W. Yang, J. Yu, Z. Li, C. Tao, Fixed-time prescribed performance adaptive trajectory tracking control for a QUAV, *IEEE Trans. Circuits Syst. II Express Briefs*, **69**(2):494–498, 2022, <https://doi.org/10.1109/TCSII.2021.3084240>.
6. L. Ding, W. Sun, Neuroadaptive prescribed-time secure control for nonlinear interconnected NCSs via multiple triggering against DoS attacks, *Appl. Math. Comput.*, **470**:128562, 2024, <https://doi.org/10.1016/j.amc.2024.128562>.
7. S. M. Esmaili, R. Zahedifar, A. Keymasi-Khalaji, Fault-tolerant fixed-time prescribed performance control of MEMS gyroscope, *IET Control. Theory Appl.*, **17**(11):1509–1521, 2023, <https://doi.org/10.1049/cth2.12484>.
8. S. S. Ge, F. Hong, T. H. Lee, Adaptive neural control of nonlinear time-delay systems with unknown virtual control coefficients, *IEEE Trans. Cybern.*, **34**(1):499–516, 2004, <https://doi.org/10.1109/TSMCB.2003.817055>.
9. X. Guo, H. Zhang, J. Sun, Y. Zhou, Fixed-time fuzzy adaptive control of manipulator systems under multiple constraints: A modified dynamic surface control approach, *IEEE Trans. Syst. Man Cybern.: Syst.*, **53**(4):2522–2532, 2023, <https://doi.org/10.1109/TSMC.2022.3212988>.
10. W. He, W. Xu, X. Ge, Q.-L. Han, W. Du, F. Qian, Secure control of multiagent systems against malicious attacks: A brief survey, *IEEE Trans. Ind. Inf.*, **18**(6):3595–3608, 2022, <https://doi.org/10.1109/TII.2021.3126644>.
11. C. Hua, H. Li, K. Li, W. Ding, Low-computation tracking control of nonlinear systems with asymmetric full-state constraints and unknown control directions, *IEEE Trans. Syst. Man Cybern.: Syst.*, **53**(2):1051–1059, 2023, <https://doi.org/10.1109/TSMC.2022.3191789>.
12. Y. Li, S. Tong, L. Liu, G. Feng, Adaptive output-feedback control design with prescribed performance for switched nonlinear systems, *Automatica*, **80**:225–231, 2017, <https://doi.org/10.1016/j.automatica.2017.02.005>.
13. T. Liu, Z. Qin, Y. Hong, Z.-P. Jiang, Distributed optimization of nonlinear multiagent systems: A small-gain approach, *IEEE Trans. Autom. Control*, **67**(2):676–691, 2022, <https://doi.org/10.1109/TAC.2021.3053549>.
14. Y. Liu, H. Ma, Adaptive fuzzy tracking control of nonlinear switched stochastic systems with prescribed performance and unknown control directions, *IEEE Trans. Syst. Man Cybern.: Syst.*, **50**(2):590–599, 2020, <https://doi.org/10.1109/TSMC.2017.2764685>.
15. H. Min, S. Xu, B. Zhang, Q. Ma, D. Yuan, Fixed-time Lyapunov criteria and state-feedback controller design for stochastic nonlinear systems, *IEEE/CAA J. Autom. Sin.*, **9**(6):1005–1014, 2022, <https://doi.org/10.1109/JAS.2022.105539>.
16. A. Polyakov, Nonlinear feedback design for fixed-time stabilization of linear control systems, *IEEE Trans. Autom. Control*, **57**(8):2106–2110, 2012, <https://doi.org/10.1109/TAC.2011.2179869>.
17. X. Qi, C. Yang, S. Xu, Adaptive fixed-time tracking control for uncertain nonlinear systems with unknown control coefficients and prescribed performance, *Inf. Sci.*, **662**:120152, 2024, <https://doi.org/10.1016/j.ins.2024.120152>.

18. C. Qian, W. Lin, A continuous feedback approach to global strong stabilization of nonlinear systems, *IEEE Trans. Autom. Control*, **46**(7):1061–1079, 2001, <https://doi.org/10.1109/9.935058>.
19. L. Shao, W. Sun, L. Ding, Finite-time adaptive control of output constrained nonlinear systems under deception attacks, *Nonlinear Dyn.*, **112**(19):17273–17290, 2024, <https://doi.org/10.1007/s11071-024-09951-8>.
20. A. Sharghi, B. Karimi, S.M. Dehghan, Fixed-time adaptive tracking control of two moving targets for a class of non-linear multi-agent systems, *Inf. Sci.*, **648**:119503, 2023, <https://doi.org/10.1016/j.ins.2023.119503>.
21. R. Singh, J. Keshavan, Approximation-free robust tracking control of unknown redundant manipulators with prescribed performance and input constraints, *IEEE Trans. Syst. Man Cybern.: Syst.*, **54**(11):6743–6755, 2024, <https://doi.org/10.1109/TSMC.2024.3444030>.
22. W. Sun, L. Ding, Y. Li, D. Yu, Decentralized adaptive secure control of nonlinear NCSs under hybrid attacks via event-triggering, *IEEE Trans. Cybern.*, **55**(8):3974–3986, 2025, <https://doi.org/10.1109/TCYB.2025.3567457>.
23. W. Sun, Z. Wang, X. Lv, F. E. Alsaadi, H. Liu, H_∞ observer design for networked Hamiltonian systems with sensor saturations and missing measurements, *Inf. Sci.*, **593**:577–590, 2022, <https://doi.org/10.1016/j.ins.2022.02.010>.
24. C. Wang, D. J. Hill, S. S. Ge, G. Chen, An ISS-modular approach for adaptive neural control of pure-feedback systems, *Automatica*, **42**(5):723–731, 2006, <https://doi.org/10.1016/j.automatica.2006.01.004>.
25. F. Wang, G. Lai, Fixed-time control design for nonlinear uncertain systems via adaptive method, *Syst. Control Lett.*, **140**:104704, 2020, <https://doi.org/10.1016/j.sysconle.2020.104704>.
26. Y.-L. Wang, Q.-L. Han, Network-based modelling and dynamic output feedback control for unmanned marine vehicles in network environments, *Automatica*, **91**:43–53, 2018, <https://doi.org/10.1016/j.automatica.2018.01.026>.
27. T. Xu, Z. Duan, Z. Sun, G. Chen, Distributed fixed-time coordination control for networked multiple Euler-Lagrange systems, *IEEE Trans. Cybern.*, **52**(6):4611–4622, 2022, <https://doi.org/10.1109/TCYB.2020.3031887>.
28. S. J. Yoo, Neural-network-based adaptive resilient dynamic surface control against unknown deception attacks of uncertain nonlinear time-delay cyberphysical systems, *IEEE Trans. Neural Networks Learn. Syst.*, **31**(10):4341–4353, 2020, <https://doi.org/10.1109/TNNLS.2019.2955132>.
29. K. Zhao, Y. Song, C. L. P. Chen, L. Chen, Adaptive asymptotic tracking with global performance for nonlinear systems with unknown control directions, *IEEE Trans. Autom. Control*, **67**(3):1566–1573, 2022, <https://doi.org/10.1109/TAC.2021.3074899>.